The Accuracy of the EASI-Derived Spatial QRS-T Angle

Daniel Guldenring, Dewar D Finlay, Raymond R Bond, Alan Kennedy, James McLaughlin

University of Ulster, Belfast, United Kingdom

Abstract

There has been recent interest in whether the spatial QRS-T angle (SA) can be used in Thorough QT studies to serve as a marker for increased risk of torsades de pointes. The determination of the SA requires vectorcardiographic data. Such data is however seldom recorded in monitoring applications. Specifically the number and the location of the electrodes, that are required when recording the Frank VCG, complicate the recording of vectorcardiographic data in monitoring applications. An alternative and more practical way for obtaining vectorcardiographic data in monitoring applications is the utilization of the EASI lead system. A previously published set of linear lead transformations allows for the derivation of the Frank VCG from the EASI lead system. This EASI-derived VCG can be used for the determination of an EASI-derived SA (ESA). The accuracy of the ESA has, however, not been reported in the literature. The aim of this research was the quantification of the differences between the ESA and the SA. This was achieved using electrocardiographic data recorded from 220 healthy subjects. To this end, the difference (ESA-SA) between the ESA and the SA was calculated for all 220 subjects. This difference was subsequently analyzed in order to determine the systematic error (mean difference) and the random error (span of the Bland- Altman 95% limits of agreement) that is made when determining the ESA. The systematic error between the SA and the ESA was found to be 11.6° [95% confidence interval: 9.8°; 13.40°]. The random error was found to be 52.9° [95% confidence interval: 48.44°; 58.45°]. The findings of this research suggest that both systematic and random error can not be overlooked when using the ESA as a substitute for the SA.

1. Introduction

The regulatory authority members of the 'International Conference on Harmonization of Technical Requirements for Registration of Pharmaceuticals for Human Use' require that all new drugs with systemic bio-availability have to undergo a so called Thorough QT study (TQT) [1]. The aim of such a TQT study is the identification of non-antiarrhythmic drugs that prolong the cardiac repolarization [2]. The heart-rate corrected QT interval (QTc) is, in TQT studies, commonly used as a surrogate marker for a prolonged cardiac repolarization and an associated increased arrhythmic risk of drugs. However, the QTc is widely viewed as a poor surrogate marker for increased arrhythmic risk of drugs [3]. This is because the QTc is not able to differentiate benign from malignant prolongations of the QTc [4]. Using the QTc prolongation as a marker for torsades de pointes (TdP) risk can therefore lead to the mischaracterization of some drugs as leading to an increased risk of TdP. This is undesired as this could stop the development of potentially useful drugs in an early phase of development [1]. Alternative and/or complementary markers for the identification of malignant QTc prolongation are therefore needed [1, 4, 5]. The vectorcardiographic parameter 'spatial QRS-T angle' (SA) has recently been proposed as a complementary marker for the identification of malignant QTc prolongation [4]. The utilization of the SA in TQT trials requires the recording of vectorcardiographic data. The requirement of vectorcardiographic data conflicts with the frequently adopted Holter monitoring strategy in TQT trials [6]. This is because the number and the location of the electrodes, that are required when recording the Frank VCG, complicate the recording of vectorcardiographic data in monitoring applications. An alternative and more practical way for obtaining vectorcardiographic data in monitoring applications is the utilization of the EASI lead system [7]. A previously published set of linear lead transformations allows for the derivation of the Frank VCG from the EASI lead system [7]. This EASI-derived VCG can be used for the determination of an EASI-derived SA (ESA). The accuracy of the ESA has, however, not previously been reported in the literature. The aim of this research was the quantification of the differences between the ESA and the SA.

2. Material and methods

2.1. ECG data

We base our research on 220 body surface potential maps (BSPMs). The BSPMs were recorded from subjects

that did not show abnormalities in their surface ECG data. Each BSPM contained electrocardiographic data of 120 leads. Three of the 120 leads were recorded from electrodes placed on the right and left wrist and the left ankle (VR, VL and VF respectively). The remaining 117 leads were recorded from thoracic electrodes (81 anterior and 36 posterior recording sites). A comprehensive description of the BSPM data and the recording procedure can be found in [8, 9]. A number of electrocardiographic leads that were required to conduct our research were associated with electrode locations that fell between the locations of the 117 thoracic electrodes. The electrocardiographic data of such leads was obtained using a previously described two-step interpolation procedure [10]. First, the 117 lead BSPMs were transformed into 352 lead BSPMs. This was performed using a Laplacian 3D interpolation method [11]. The location of the 352 thoracic leads corresponded to the nodes in the Dalhousie torso [12]. Second, any required thoracic leads that were located between the 352 thoracic leads were obtained using linear interpolation [13].

2.2. Generation of the Frank VCG

The potentials at the A, C, E, F, H, I and M electrode locations of the Frank lead system [14], were extracted from the BSPMs. The potentials at the Frank electrode locations were used to derive the Frank VCG using (1).

$$\boldsymbol{VCG^{Frank}} = \boldsymbol{A^{Frank}} \cdot \begin{bmatrix} \boldsymbol{\varphi_A} \\ \vdots \\ \boldsymbol{\varphi_M} \end{bmatrix}. \quad (1)$$

Where $\boldsymbol{\varphi_A}$, $\boldsymbol{\varphi_C}$, $\boldsymbol{\varphi_E}$, $\boldsymbol{\varphi_F}$, $\boldsymbol{\varphi_H}$, $\boldsymbol{\varphi_I}$, and $\boldsymbol{\varphi_M}$ are $1 \times N$ vectors that contain N sample values of potentials at the Frank electrode locations A to M respectively, $\boldsymbol{A^{Frank}}$ is a 3×7 matrix of published coefficients [15] that allow for a derivation of the Frank VCG using the potentials $\boldsymbol{\varphi_A}$ to $\boldsymbol{\varphi_M}$, and $\boldsymbol{VCG^{Frank}}$ is a $3\times N$ matrix containing N sample values of the three Frank leads X, Y and Z.

2.3. Generation of the EASI-derived VCG

The three EASI leads ES, AS and AI were extracted from the BSPMs. The three EASI leads were used to derive the Frank VCG using (2).

$$\boldsymbol{VCG^{EASI}} = \boldsymbol{A^{EASI}} \cdot \begin{bmatrix} \boldsymbol{ES} \\ \boldsymbol{AS} \\ \boldsymbol{AI} \end{bmatrix}. \quad (2)$$

Where $\boldsymbol{ES}$, $\boldsymbol{AS}$, and $\boldsymbol{AI}$ are $1 \times N$ vectors that contain N sample values of the EASI leads ES, AS and AI respectively, $\boldsymbol{A^{EASI}}$ is a 3×3 matrix of published coefficients [7, Table 2] that allow for the derivation of the EASI-derived VCG using three EASI leads and $\boldsymbol{VCG^{EASI}}$ is a $3\times N$ matrix containing N sample values of the three EASI-derived VCG leads X, Y and Z.

2.4. Determination of the spatial QRS-T angle

The SA and the ESA were calculated as detailed in (3) to (6).

$$\boldsymbol{QRS_m^d} = \frac{1}{J_p - QRS_{ON}} \sum_{n=QRS_{ON}}^{J_P} \boldsymbol{VCG^d}(n). \quad (3)$$

$$\boldsymbol{T_m^d} = \frac{1}{T_{END} - J_P} \sum_{n=J_P}^{T_{END}} \boldsymbol{VCG^d}(n). \quad (4)$$

$$SA = arccos\left[\frac{\boldsymbol{QRS_m^{Frank}} \cdot \boldsymbol{T_m^{Frank}}}{|\boldsymbol{QRS_m^{Frank}}| \cdot |\boldsymbol{T_m^{Frank}}|}\right]. \quad (5)$$

$$ESA = arccos\left[\frac{\boldsymbol{QRS_m^{EASI}} \cdot \boldsymbol{T_m^{EASI}}}{|\boldsymbol{QRS_m^{EASI}}| \cdot |\boldsymbol{T_m^{EASI}}|}\right]. \quad (6)$$

Where $\boldsymbol{QRS_m^d}$ is the 3×1 mean vector of ventricular depolarization, $\boldsymbol{T_m^d}$ denotes the 3×1 mean vector of ventricular repolarization, QRS_{ON} is the sample index of the QRS onset, J_P denotes the sample index of the J-point, T_{END} is the sample index associated with the end of the T wave, $\boldsymbol{VCG^d}$ is a $3\times N$ matrix containing N sample values of the three VCG leads and $d \in \{Frank, EASI\}$ indicates whether a parameter is derived using the Frank lead system or the EASI lead system.

2.5. Performance assessment

The performance assessment was conducted using the differences between ESA and SA. These differences were calculated as detailed in (7).

$$\Delta\boldsymbol{SA} = \boldsymbol{ESA} - \boldsymbol{SA}. \quad (7)$$

Where $\boldsymbol{ESA}$ and $\boldsymbol{SA}$ are vectors that contain the ESA and the SA values of all subjects in the study population and $\Delta\boldsymbol{SA}$ is a vector that contains the differences between the ESA and the SA values of all subjects in the study population.

First, the distribution of the elements in $\Delta\boldsymbol{SA}$ was analysed using a histogram. Second, the systematic and the random error component of the differences between ESA and SA were analyzed. The systematic error was quantified as mean [95% confidence intervals (CI)] of the elements in $\Delta\boldsymbol{SA}$. We quantified the random error using the span of the Bland-Altman (BA) 95% limits of agreement [16] as detailed in (8).

$$\text{RandomError} = \boldsymbol{2 \cdot 1.96 \cdot std}(\Delta\boldsymbol{SA}). \quad (8)$$

Where $\boldsymbol{std}(\cdot)$ denotes the standard deviation and $\Delta\boldsymbol{SA}$ is as defined in (7).

Third, a Breusch-Pagan (BP) test [17] was conducted to assess whether the variance of the differences between ESA and SA is dependent upon the SA value. Forth, the strength of the linear relationship between ESA and SA was quantified using the sample Pearson correlation coefficient. Fifth, we developed a linear model in an attempt to reduce the difference between ESA and SA. Sixth, the performance of the linear model in reducing the differences between ESA and SA was assessed.

3. Results

A histogram that details the distributional character of the elements in $\Delta\boldsymbol{SA}$ is depicted in Figure 1.

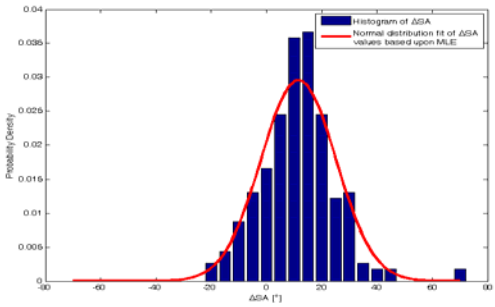

Figure 1. Histogram of the elements in $\Delta\boldsymbol{SA}$ and maximum likelihood normal distribution fit of the $\Delta\boldsymbol{SA}$ values.

It can be seen from Figure 1 that the histogram of the elements in $\Delta\boldsymbol{SA}$ is well described by a maximum likelihood normal distribution fit.

The analysis of the elements in $\Delta\boldsymbol{SA}$ found a systematic error of 11.6° [95% CI: 9.81°; 13.40°] and a random error of 52.97° [95% CI: 48.44°; 58.44°]. Both systematic and random error can be seen in the BA plot that is depicted in Figure 2.

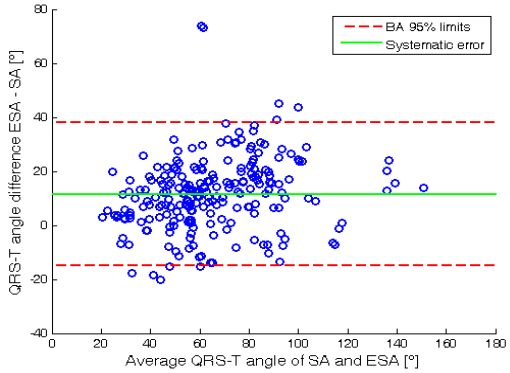

Figure 2. Bland-Altman plot of the differences between ESA and SA over the average angle between ESA and SA.

The distribution of the elements in $\Delta\boldsymbol{SA}$, that is depicted in Figure 2, suggests a constant magnitude of the error variance across the codomain $\{0° \leq SA \leq 180°\}$ of the SA. The linear dependence of the error variance (variance of the difference ESA-SA) from the SA value was formally assessed using the BP test. No evidence p = 0.25 for a linear relationship between the error variance and the SA value was found based upon the BP test. This finding and the distribution of the $\Delta\boldsymbol{SA}$ values in Figure 2 indicate that the magnitude of the random error can be considered constant across the entire codomain of the SA.

The scatter plot in Figure 3 depicts the relationship between the SA and the ESA.

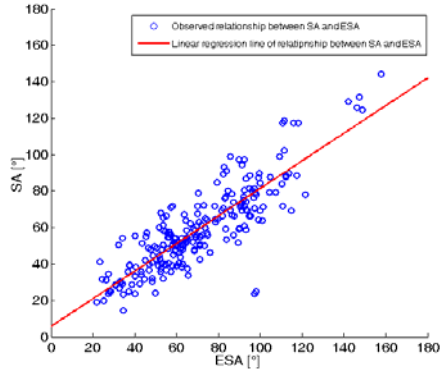

Figure 3. Scatter plot and least-squares fit linear regression line of the relationship between ESA and SA based upon data of all subjects in the study population.

The scatter plot in Figure 3 does suggest a linear relationship between ESA and SA. The strength of this linear relationship was quantified to be 0.854 [95% CI: 0.813; 0.886] using the sample Pearson correlation coefficient.

The linear model in (9) was designed to assess whether a linear transformation can reduce the magnitude of systematic error and random error when estimating the SA using the EASI lead system.

$$LESA = b_0 + b_1 \cdot ESA. \qquad (9)$$

Where $LESA$ is an estimate of the SA based upon the linear transformation of an observed ESA value, b_0 is the intercept and b_1 is the slope of the linear model.

The model parameters b_0 and b_1 of (9) were derived using least-squares linear regression analysis. The conducted regression analysis was performed using the data of the study population and 10-fold cross-validation. Both the systematic error and the random error based upon the SA estimation methods in (6) and in (9) were quantified for each of the 10 folds. The observed error magnitudes as well as the linear model parameters of (9) are detailed in Table 1.

Table 1. Linear model parameters and error magnitudes for ESA and LESA estimates of the SA.

Parameter	Sample value	95% confidence interval
Rand. err. ESA-SA [°]	51.99	[43.03; 60.95]
Rand. err. LESA-SA [°]	46.31	[38.04; 54.57]
Syst. err. ESA-SA [°]	11.60	[9.90; 13.31]
Syst. err. LESA-SA [°]	-0.014	[-1.81; 1.78]
b_0 [°]	5.41	[4.91; 5.92]
b_1*	0.761	[0.753; 0.769]

*dimensionless

The null hypothesis of identical estimation errors in ESA and LESA estimates was assessed using the paired two-sample t-test. This was performed for both the systematic error and the random error. The paired two-sample t-test indicated a statistically significant difference between systematic error p<0.001 and the random error p<0.001 of both SA estimation methods. Both p-values

lead to a rejection of the null hypothesis and indicate that the LESA estimates are associated with lower systematic and random errors when compared to ESA estimates.

4. Discussion

In this paper we reported on the similarity between the SA and the ESA.

Our findings have shown that the utilization of the ESA as a substitute for the SA is associated with both random and systematic error. Further analysis of the relationship between SA and ESA has shown that a linear regression model can be used to reduce systematic and random error. The utilization of the developed linear regression model resulted, however, only in minor reduction of the random error from 51.99° [95% CI: 43.03°; 60.95°] to 46.31° [95% CI: 38.04°; 54.57°]. The observed magnitude of the random error raises questions about the suitability of the ESA as a substitute for the SA.

It is necessary to stress that our research has assessed the SA estimation performance of the EASI lead system using a transformation matrix $\boldsymbol{A^{EASI}}$ that has not been optimized for SA monitoring applications. Further research should therefore assess the possibility of improving the SA estimation performance of the EASI lead system by designing a transformation matrix that is optimized for the estimation of the repolarization parameter SA.

The normal limits of the SA variability during baseline and during drug arms of TQT trials are, in addition to the absolute values of SA and ESA, of potential interest for the quantification of repolarization changes. Further research should therefore assess the differences in the variability of SA and ESA during baseline and during drug arms of TQT trials.

5. Conclusion

The findings of our research suggest that both systematic and random error cannot be overlooked when using the ESA as a substitute for the SA. Especially the relatively large random error raises questions about the utility of the ESA as a substitute for the SA.

Acknowledgements

This work has been supported by the Northern Ireland Connected Health Innovation Centre.

References

[1] Salvi V, Karnad DR, Panicker GK, Kothari S. Update on the evaluation of a new drug for effects on cardiac repolarization in humans: issues in early drug development. Br J Pharmacol 2010; 159: 34-48.

[2] Shah RR. Drugs, QTc interval prolongation and final ICH E14 guideline: an important milestone with challenges ahead. Drug Saf 2005; 28: 1009-1028.

[3] Kowey PR, Malik M. The QT interval as it relates to the safety of non-cardiac drugs. Eur Heart J 2007;9 Suppl G:G3-G8.

[4] Johannesen L, Vicente J, Galeotti L, Loring Z, Florian JA, Garnett CE, et al. Abstract 15725: Normal Limits of Variability of Spatial QRS-T Angle and Ventricular Gradient: Analysis of 20 Thorough-QT Studies. Circulation 2012; 126:A15725.

[5] Kligfield P. Electrocardiography and repolarization abnormalities in cardiac safety: Benefits and limitations of fully automated methods for QT measurement. Comp Cardiol 2010; 37:253-256.

[6] Couderc J, Garnett C, Li M, Handzel R, McNitt S, Xia X, et al. Highly Automated QT Measurement Techniques in 7 Thorough QT Studies Implemented under ICH E14 Guidelines. Ann Noninvasive Electrocardiol 2011; 16:13-24.

[7] Field DQ, Feldman CL, Horáček BM. Improved EASI coefficients: Their derivation, values, and performance. J Electrocardiol 2002; 35 Suppl:23-33.

[8] Kornreich F, Montague T, Rautaharju P. Identification of first acute Q wave and non-Q wave myocardial infarction by multivariate analysis of body surface potential maps. Circulation 1991; 84: 2442-2453.

[9] Montague TJ, Smith ER, Cameron DA, Rautaharju PM, Klassen GA, Felmington CS, et al. Isointegral analysis of body surface maps: surface distribution and temporal variability in normal subjects. Circulation, 1981; 63: 1166-1172.

[10] Finlay DD, Nugent CD, Nelwan SP, Bond RR, Donnelly MP, Guldenring D. Effects of electrode placement errors in the EASI-derived 12-lead electrocardiogram. J Electrocardiol 2010; 43: 606-611.

[11] Oostendorp TF, van Oosterom A, Huiskamp G. Interpolation on a triangulated 3D surface. J Comput Phys 1989; 80:331-343.

[12] Horáček BM. Numerical Model of an Inhomogeneous Human Torso. Adv Cardiol 1974; 10:51-57.

[13] Schijvenaars BJA, Kors JA, van Herpen G, Kornreich F, van Bemmel JH. Interpolation of body surface potential maps. J Electrocardiol 1995; 28 Suppl 1: 104-109.

[14] Frank E. An accurate, clinically practical system for spatial vectorcardiography. Circulation 1956; 13:737-749.

[15] Macfarlane PW. Lead systems. In: Macfarlane PW, van Oosterom A, Pahlm O, Kligfield P, Janse M, Camm J, editors. Comprehensive Electrocardiology. 2nd ed. United Kingdom. London: Springer; 2011; 375-426.

[16] Bland JM, Altman DG. Statistical methods for assessing agreement between two methods of clinical measurement. Lancet 1986; 1(8476):307-310.

[17] Breusch TS, Pagan AR. Simple Test for Heteroscedasticity and Random Coefficient Variation. Econometrica 1979; 47:1287-1294.

Address for correspondence.

Daniel Guldenring
Room 25A03, School of Engineering, University of Ulster,
Shore Road, Newtownabbey, Co. Antrim, BT37 0QB
guldenring-d2@email.ulster.ac.uk